Specialty Journal of Pharmacognosy, Phytochemistry, and Biotechnology
ISSN: 3062-441X
2022, Volume 2, Page No: 126-141

Available online at: www.galaxypub.co/page/journals

Galaxy Publication

Galaxy Publication

Investigating the Effects of Astragalus Polysaccharide on Immune Cell Infiltration and Prognostic Biomarker Improvement in Pediatric Acute Myeloid Leukemia

Anil Deshpande[1], Mahesh Joshi[1], Rajesh Kulkarni[1], Vikram Pawar[1], Suresh Patil[1]*

[1]Department of Pharmacognosy, Faculty of Pharmacy, Savitribai Phule Pune University, Pune, India.

***E-mail** ✉ suresh.patil.pg@gmail.com

Received: 12 February 2022; **Revised:** 21 May 2022; **Accepted:** 23 May 2022

ABSTRACT

Acute myeloid leukemia (AML) is a major form of cancer in children, yet treatment strategies remain limited and outcomes suboptimal. This study explored how Astragalus polysaccharide (APS) might influence immune cell dynamics and prognostic markers in pediatric AML. Gene expression data from the GEO dataset GSE2191 were analyzed to identify differentially expressed genes (DEGs), while APS-associated genes (APSRGs) were retrieved from the Swiss Target Prediction platform. Overlapping DEGs and APSRGs ($|logFC| > 1$, $p < 0.05$) were defined as APS-related DEGs (APSRDEGs) and visualized with a Venn diagram. Protein-protein interaction (PPI) networks were constructed to pinpoint key hub genes. Functional enrichment via Gene Ontology (GO) and KEGG pathways was performed to determine the biological roles, molecular functions, cellular locations, and pathways linked to these hub genes. Associations with pediatric AML were further assessed through correlation analysis, ROC curves, and immune infiltration profiling. Comparison between pediatric AML and control samples identified 1,881 DEGs, among which 20 were APSRDEGs. PPI network mapping revealed 13 interconnected APSRDEGs, from which nine hub genes were highlighted: CASP3, PTPRC, ELANE, HMOX1, CHUK, FLT1, JAK3, CTSL, and AURKA. GO and KEGG analyses indicated that these hub genes are involved in critical biological processes and pathways relevant to AML pathogenesis. ROC curve evaluation demonstrated significant differential expression of the hub genes between AML and control groups. Immune infiltration analysis revealed notable correlations between hub gene expression and immune cell presence, with HMOX1 showing the strongest positive association with neutrophils. Nine APS-associated hub genes were identified in pediatric AML, suggesting that APS may modulate immune infiltration and affect disease prognosis. These results point to APS as a promising candidate for therapeutic intervention in pediatric AML.

Keywords: APS, Prognostic biomarker, Pediatric acute myeloid leukemia (PAML), PPI network, GEO database, immune infiltration analysis

How to Cite This Article: Deshpande A, Joshi M, Kulkarni R, Pawar V, Patil S. Investigating the Effects of Astragalus Polysaccharide on Immune Cell Infiltration and Prognostic Biomarker Improvement in Pediatric Acute Myeloid Leukemia. J Pharmacogn Phytochem Biotechnol. 2022;2:126-41. https://doi.org/10.51847/Kg0WtkaFEt

Introduction

Acute myeloid leukemia (AML) is a hematologic malignancy marked by excessive proliferation of immature myeloid cells, which disrupts normal hematopoiesis. In children, AML represents nearly one-fifth of all leukemia diagnoses, posing a persistent therapeutic challenge despite advances in intensive chemotherapy and hematopoietic stem cell transplantation [1]. A critical issue in pediatric AML management is the frequent relapse observed in one-third to one-half of patients following initial remission [2]. This recurrence is largely attributed to leukemic stem cells that survive conventional therapy, emphasizing the urgent need for complementary or alternative strategies to improve long-term outcomes.

Astragalus polysaccharide (APS), a bioactive constituent of the traditional Chinese herb Astragalus membranaceus, has attracted attention due to its broad pharmacological effects, including immune regulation and anti-cancer activity. While APS has been studied extensively in solid tumors such as colorectal, hepatic, pulmonary, and gastric cancers, its role in leukemia—especially pediatric AML—remains largely unexplored.

Evidence indicates that APS can suppress tumor proliferation, migration, and invasion by influencing signaling pathways that govern apoptosis, cell growth, and immune responses. For instance, APS has been reported to induce apoptosis in cancer cell lines, including colon and breast cancers, through activation of intrinsic apoptotic pathways and downregulation of anti-apoptotic proteins [3].

In the context of leukemia, APS shows promise in modulating the tumor immune microenvironment. Studies suggest that APS enhances the anti-leukemic immune response by promoting the proliferation and cytotoxic activity of natural killer (NK) cells and T lymphocytes. Furthermore, APS may alleviate leukemia-associated inflammation, potentially mitigating chemotherapy-related toxicity and enhancing therapeutic efficacy.

Despite current standard treatments such as chemotherapy and stem cell transplantation, challenges such as drug resistance, systemic toxicity, and high relapse rates remain significant. APS, with its multi-targeted effects on apoptosis, immune modulation, and inflammation, presents a promising adjunct therapy. However, the precise molecular mechanisms through which APS exerts its anti-leukemic effects in pediatric AML are still not fully defined.

Network pharmacology offers a systemic approach to investigating interactions between multiple molecular targets, making it an effective strategy to identify potential therapeutic pathways and targets in complex diseases [4] Given that leukemia involves multi-gene regulatory networks, network pharmacology is particularly well-suited for identifying actionable targets. In this study, we combined GEO-derived pediatric AML gene expression data with APS-related target genes (APSRGs) obtained via the SwissTargetPrediction platform. Differentially expressed genes (DEGs) were identified and intersected with APSRGs to define APS-related DEGs (APSRDEGs). Hub genes were determined using protein-protein interaction (PPI) networks, and their functional relevance was explored via Gene Ontology (GO) and KEGG enrichment analyses. Finally, ROC curve analysis and immune infiltration profiling were employed to evaluate the diagnostic and prognostic significance of these hub genes, ultimately identifying APS-associated candidates that may modulate immune responses and serve as biomarkers in pediatric AML.

Materials and Methods

Data acquisition

Gene expression data for pediatric AML were retrieved from the Gene Expression Omnibus (GEO) database (http://www.ncbi.nlm.nih.gov/geo/) [5]. The dataset GSE2191 [6] was selected, consisting of human bone marrow and peripheral blood samples. This dataset was generated on the GPL8300 platform, with sample information summarized in **Table 1**. A total of 54 pediatric AML samples and 4 control samples were included in this analysis. Data preprocessing steps—such as probe annotation, normalization, and standardization—were performed using the limma R package [7]. Boxplots were generated to visualize expression distributions before and after normalization, ensuring consistency across samples.

Table 1. GEO microarray chip information.

	GSE2191
Platform	GPL8300
Type	Array
Species	*Homo sapiens*
Tissue	Bone marrow or peripheral blood
Samples in the PAML group	54
Samples in the Control group	4
Reference	PMID: 12738660

GEO, gene expression omnibus; PAML, pediatric acute myeloid leukemia.

Prediction of astragalus polysaccharide targets

To explore the molecular interactions of Astragalus polysaccharide (APS), its chemical profile, including the SMILES notation, was retrieved from the PubChem database (https://pubchem.ncbi.nlm.nih.gov/) [8]. Potential targets of APS (APSRGs) were predicted using the SwissTargetPrediction platform

(http://swisstargetprediction.ch/) [9], which evaluates likely interactions based on the chemical structure. To visualize these relationships, an APS-target interaction network was constructed, illustrating how APS may interact with multiple molecular targets.

Identification of APS-related differentially expressed genes in pediatric AML

The GSE2191 dataset was split into pediatric AML (PAML) and control groups for analysis. Differentially expressed genes (DEGs) were determined using the limma R package, applying thresholds of $|logFC| > 1$ and $p < 0.05$. Upregulated genes were defined by $logFC > 1$ and $p < 0.05$, while downregulated genes had $logFC < -1$ and $p < 0.05$. P-value correction was performed using the Benjamini–Hochberg (BH) method.

To focus on APS-related genes, DEGs were intersected with the predicted APSRGs. Only overlapping genes meeting the DEG criteria were retained as APS-related DEGs (APSRDEGs).

Construction of protein-protein interaction networks and hub gene selection

APSRDEGs were analyzed for protein-protein interactions using the STRING database (http://string-db.org/) [10] with a minimum confidence threshold of 0.400. Subnetworks corresponding to potential functional clusters were extracted for further study. Hub genes were identified using the CytoHubba plugin in Cytoscape [11, 12] by applying five ranking algorithms: Maximal Clique Centrality (MCC), Maximum Neighborhood Component (MNC), Degree, Edge Percolated Component (EPC), and Closeness [13]. Genes consistently ranked in the top positions across all five methods were considered hub genes, with overlap visualized through a Venn diagram.

Functional enrichment analysis

To interpret the biological roles of hub genes, Gene Ontology (GO) analysis [14] was performed, encompassing biological processes (BP), cellular components (CC), and molecular functions (MF). KEGG pathway analysis [15] was conducted to map hub genes to known signaling and disease pathways. Both analyses utilized the clusterProfiler R package [16]. Significance thresholds were set at adjusted p-value < 0.05 and FDR (q-value) < 0.25, with BH correction applied.

Validation of hub Gene expression and ROC analysis

Expression levels of hub genes were compared between PAML and control samples using group comparison plots. The diagnostic utility of these genes was evaluated using ROC curves via the pROC R package, with area under the curve (AUC) values interpreted as follows: >0.9 (high accuracy), 0.7–0.9 (moderate accuracy), and 0.5–0.7 (low accuracy).

Correlation and functional similarity analysis

Spearman correlation coefficients were computed to assess pairwise relationships among hub genes in GSE2191. Correlations were classified as weak/no ($|r| < 0.3$), weak ($0.3 \leq |r| < 0.5$), moderate ($0.5 \leq |r| < 0.8$), or strong ($|r| \geq 0.8$). Functional similarities were calculated using GOSemSim [17], which quantifies similarity based on GO annotations.

Immune infiltration profiling

Single-sample gene set enrichment analysis (ssGSEA) [18] was used to quantify immune cell infiltration in each sample. Correlations between hub gene expression and immune cell levels were assessed using Spearman analysis to explore potential immunomodulatory roles.

Statistical methods

All analyses were conducted in R (v4.3.0). Two-group comparisons used Student's t-test for normally distributed variables and Mann–Whitney U test for non-normal variables. For comparisons involving three or more groups, the Kruskal–Wallis test was applied. Spearman correlation was used for association studies. Significance was defined as a two-sided $p < 0.05$ unless otherwise specified.

Results and Discussion

Study workflow

The overall study design is depicted in **Figure 1**. The workflow began with identification of DEGs from GSE2191, followed by integration with APS-predicted targets from SwissTargetPrediction to generate APS-related DEGs (APSRDEGs). These genes were analyzed in a PPI network to identify hub genes. Functional enrichment, correlation analysis, immune infiltration assessment, and ROC validation were then performed to evaluate the diagnostic and prognostic relevance of hub genes in pediatric AML.

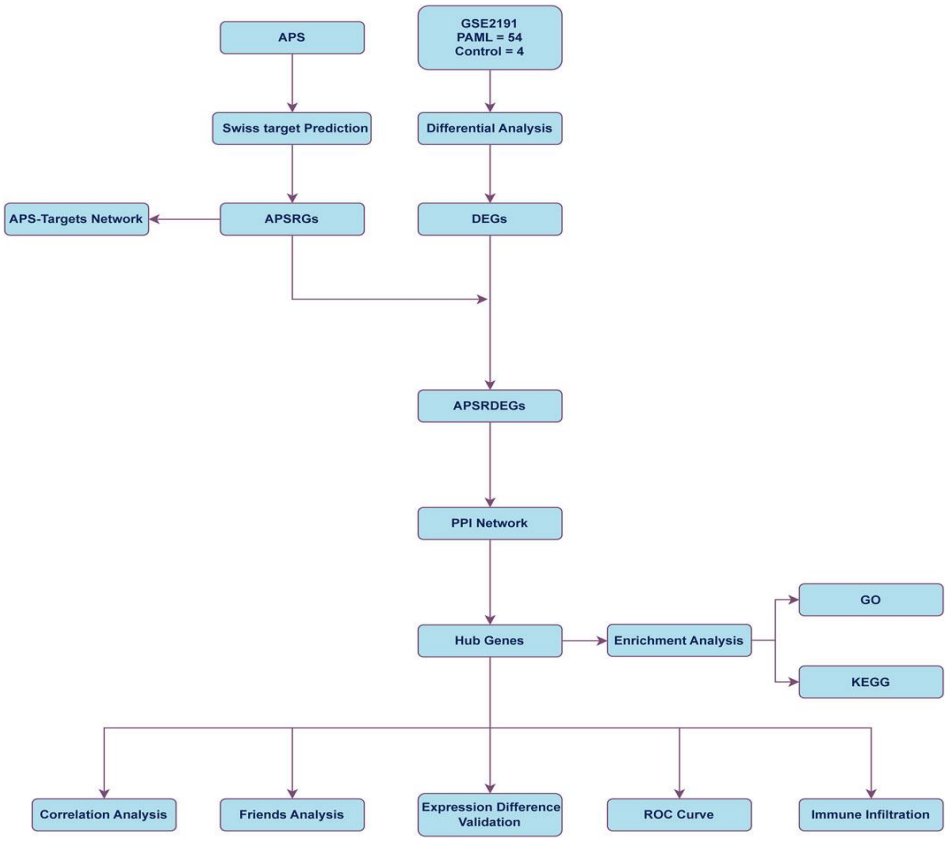

Figure 1. A Stepwise approach was implemented in this study to investigate the role of Astragalus polysaccharide (APS) in pediatric acute myeloid leukemia (PAML). The workflow begins with the identification of differentially expressed genes (DEGs) from the GSE2191 dataset, followed by integration with APS-related genes (APSRGs) predicted through SwissTargetPrediction. The overlapping genes, termed APS-related DEGs (APSRDEGs), were subjected to protein-protein interaction (PPI) network analysis to identify central hub genes. Subsequent analyses included Gene Ontology (GO) and Kyoto Encyclopedia of Genes and Genomes (KEGG) enrichment to explore the biological processes, molecular functions, and signaling pathways associated with these hub genes.

To further evaluate their clinical relevance, receiver operating characteristic (ROC) curve analyses were performed to assess diagnostic potential, while immune infiltration studies examined correlations between hub gene expression and immune cell populations. Collectively, **Figure 1** demonstrates how data acquisition, gene selection, functional enrichment, and immune-related analyses are sequentially integrated to pinpoint key biomarkers and potential therapeutic targets of APS in PAML. This schematic provides a visual representation of the study's methodology, illustrating the logical progression from initial gene identification to comprehensive functional and immunological evaluation.

Prediction of astragalus polysaccharide targets

Astragalus polysaccharide (APS) was queried in the PubChem database using its English name as the search term. As a polysaccharide composed of multiple monosaccharide units linked via glycosidic bonds, APS cannot be represented by a single fixed chemical formula. The molecular composition can vary depending on extraction methods; for instance, smaller APS molecules typically range from C18H32O16 to C24H42O21.

Potential molecular targets of APS were predicted using the SwissTargetPrediction platform, which identified 101 APS-related genes (APSRGs). These genes were mapped and visualized as a network using Cytoscape **(Figure 2)**, providing an overview of the potential molecular interactions of APS.

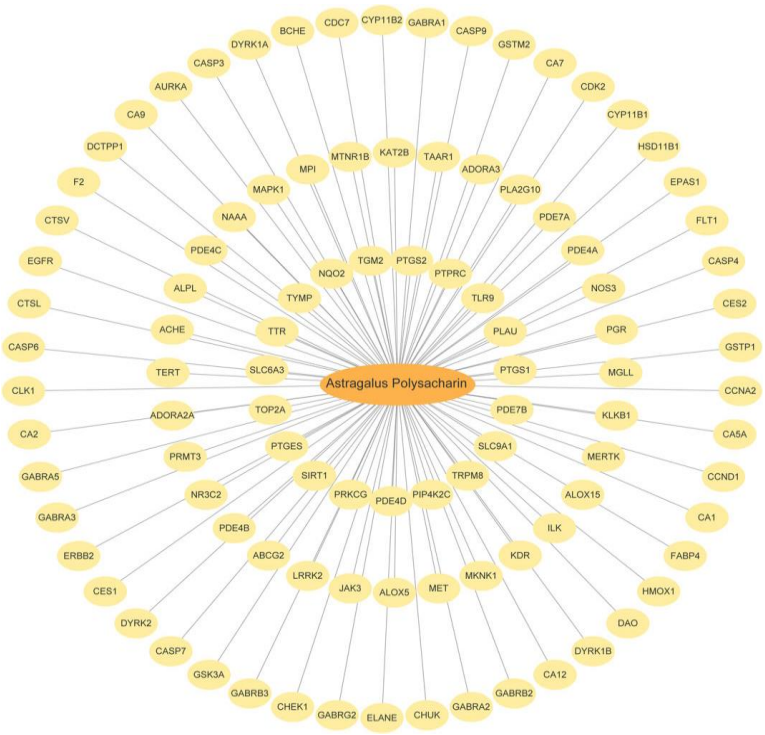

Figure 2. Interaction network between Astragalus polysaccharide (APS) and its predicted molecular targets. In the network diagram, APS is represented by the orange oval, while predicted targets from SwissTargetPrediction are shown as yellow ovals. This visual representation provides an intuitive overview of the multiple genes potentially modulated by APS, highlighting the complexity of its predicted molecular interactions.

Data standardization of pediatric AML dataset

To ensure consistency and comparability of gene expression data, the GSE2191 dataset was processed and standardized using the limma R package. Expression distributions before and after normalization were visualized through boxplots **(Figures 3a and 3b)**, demonstrating that standardization effectively minimized technical variability and prepared the dataset for downstream differential expression and integrative analyses.

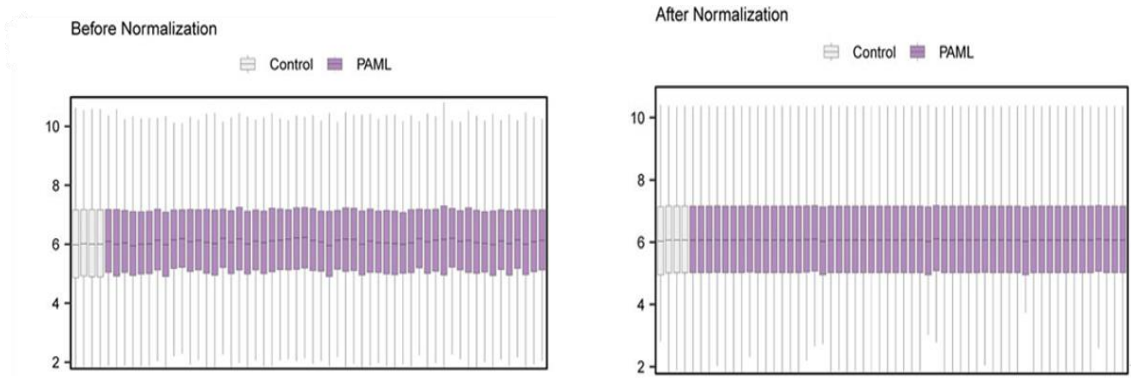

a) b)

Figure 3. GSE2191 Data Normalization. (a) Distribution of GSE2191 values before normalization is shown as a boxplot. (b) Boxplot depicting the distribution of the normalized dataset. Control samples are shown in gray, while pediatric acute myeloid leukemia (PAML) samples are in purple.

Discovery of APS-related differentially expressed genes in pediatric AML

The GSE2191 dataset was split into PAML and control cohorts, leading to the identification of 1,881 genes exhibiting significant differential expression (|logFC| > 1, p < 0.05). Of these, 1,119 genes showed increased expression, whereas 762 were downregulated. These results are visualized in a volcano plot **(Figure 4a)**.

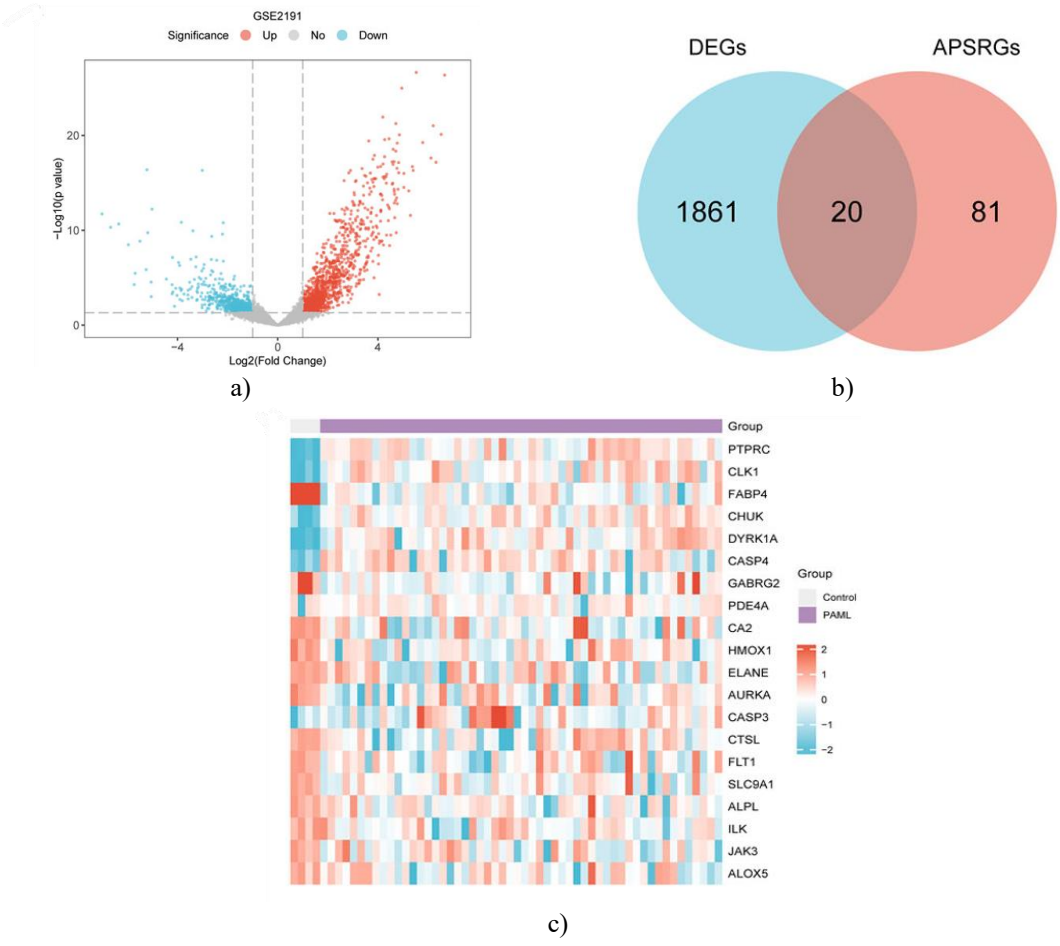

Figure 4. Differential Gene Expression Overview. (a) Volcano plot depicting genes with altered expression between PAML and control samples in the GSE2191 dataset. (b) Venn diagram showing the overlap between DEGs and APS-related genes (APSRGs). (c) Heatmap of APSRDEG expression patterns in GSE2191, with PAML samples in purple and controls in gray; red indicates elevated expression, blue indicates reduced expression, and color intensity reflects expression magnitude.

Integrating APSRGs with DEGs revealed 20 APS-associated genes (APSRDEGs), including ALOX5, ALPL, FLT1, GABRG2, HMOX1, ILK, JAK3, PDE4A, PTPRC, and SLC9A1 **(Figure 4b)**. Heatmap analysis highlighted distinct expression differences of these genes between PAML and control groups **(Figure 4c)**.

PPI Network analysis and identification of key hub genes

A protein-protein interaction (PPI) network was constructed for the 20 APSRDEGs using the STRING database. Only 13 genes exhibited strong interactions, forming a connected network: ALPL, AURKA, CA2, CASP3, CHUK, CTSL, ELANE, FABP4, FLT1, HMOX1, JAK3, PTPRC, and SLC9A1 **(Figure 5a)**. The remaining seven genes did not show significant interactions, suggesting they may function independently or indirectly.

To pinpoint the most critical genes, interaction scores were computed using five CytoHubba algorithms (MCC, MNC, Degree, EPC, Closeness). The top 10 genes from each algorithm were mapped as PPI networks **(Figures 5b–5f)**, and a Venn diagram integrating all five methods identified nine hub genes consistently highlighted across algorithms: CASP3, PTPRC, ELANE, HMOX1, CHUK, FLT1, JAK3, CTSL, and AURKA **(Figure 5g)**.

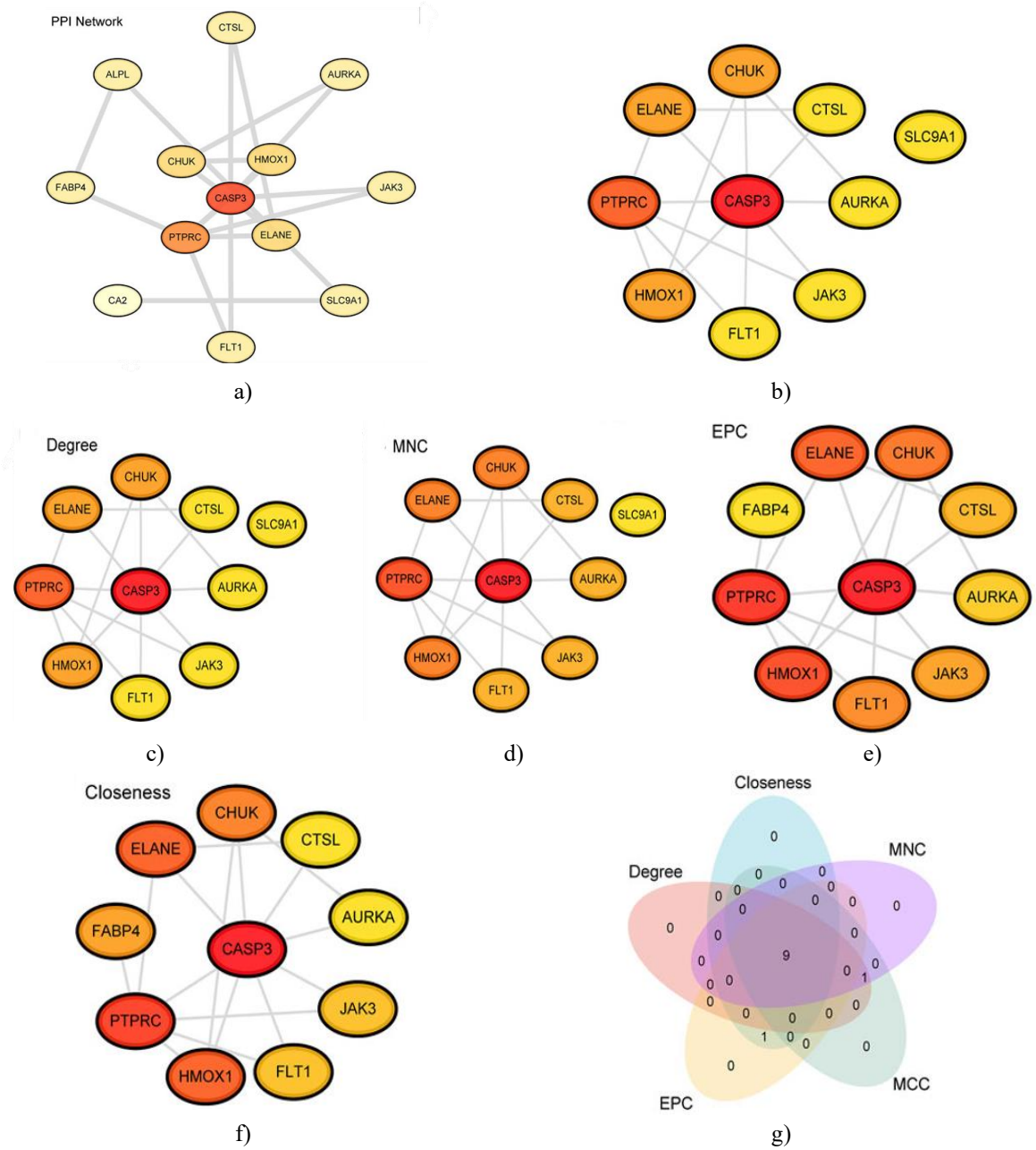

Figure 5. PPI Network Construction and Hub Gene Identification. Using the STRING database, a protein interaction map was generated for APSRDEGs, revealing that only 13 out of the 20 genes established meaningful connections, highlighting the most central players within the network (a). PPI networks of the top 10 genes were further assessed through five CytoHubba algorithms—MCC (b), MNC (c), Degree (d), EPC (e), and Closeness (f)—to determine key connectivity patterns. A Venn diagram was then used to display the genes consistently identified across all five methods, demonstrating overlapping hub genes (g).

GO and KEGG functional enrichment of hub genes

The nine hub genes were subjected to Gene Ontology (GO) and KEGG pathway enrichment to explore their functional roles, summarized in **Table 2.** Key biological processes involved modulation of leukocyte activity and immune system regulation. Cellular localization analysis indicated enrichment in structures such as membrane rafts and vacuolar lumens, while molecular functions highlighted included proteoglycan binding and proteolytic activity. KEGG pathway analysis showed these hub genes participate in apoptosis, hepatitis B, and primary immunodeficiency pathways. To better visualize these relationships, results were represented using bar and bubble plots **(Figures 6a and 6b)** and network diagrams **(Figures 6c–6f)**.

Table 2. Result of GO and KEGG enrichment analysis for hub genes.

Ontology	ID	Description	GeneRatio	BgRatio	p-value	p.adjust	q-value
BP	GO:0002695	Suppression of leukocyte activation	4/9	202/18614	1.63E-06	1.07E-03	3.63E-04
BP	GO:0050866	Inhibition of general cell activation	4/9	225/18614	2.50E-06	1.07E-03	3.63E-04
BP	GO:0002704	Downregulation of leukocyte-mediated immune responses	3/9	68/18614	3.86E-06	1.10E-03	3.73E-04
BP	GO:0002440	Generation of molecular mediators involved in immune signaling	4/9	328/18614	1.11E-05	1.89E-03	6.38E-04
BP	GO:0071900	Regulation of protein serine/threonine kinase activity	4/9	369/18614	1.77E-05	1.89E-03	6.38E-04
CC	GO:0045121	Membrane rafts	3/9	323/19518	3.50E-04	1.17E-02	6.88E-03
CC	GO:0098857	Membrane microdomains	3/9	324/19518	3.53E-04	1.17E-02	6.88E-03
CC	GO:0009898	Cytoplasmic face of the plasma membrane	2/9	159/19518	2.29E-03	4.41E-02	2.60E-02
CC	GO:0005775	Vacuolar lumen	2/9	176/19518	2.79E-03	4.41E-02	2.60E-02
CC	GO:0098562	Inner membrane surface	2/9	193/19518	3.35E-03	4.41E-02	2.60E-02
MF	GO:0043394	Binding to proteoglycans	2/9	36/18369	1.33E-04	8.66E-03	2.67E-03
MF	GO:0004175	General endopeptidase activity	3/9	428/18369	9.50E-04	2.53E-02	7.79E-03
MF	GO:0004197	Cysteine-type endopeptidase activity	2/9	118/18369	1.43E-03	2.53E-02	7.79E-03
MF	GO:0004713	Protein tyrosine kinase activity	2/9	137/18369	1.92E-03	2.53E-02	7.79E-03
MF	GO:0002020	Protease-binding capability	2/9	138/18369	1.95E-03	2.53E-02	7.79E-03
KEGG	hsa04210	Apoptosis	3/9	136/8662	2.97E-04	1.03E-02	6.33E-03
KEGG	hsa05162	Measles infection pathway	3/9	138/8662	3.10E-04	1.03E-02	6.33E-03
KEGG	hsa05418	Fluid shear stress and atherosclerosis	3/9	139/8662	3.16E-04	1.03E-02	6.33E-03
KEGG	hsa05161	Hepatitis B infection pathway	3/9	162/8662	4.97E-04	1.22E-02	7.45E-03
KEGG	hsa05340	Primary immunodeficiency	2/9	38/8662	6.62E-04	1.30E-02	7.94E-03

GO, gene ontology; BP, Biological Process; CC, Cellular Component; MF, molecular function; KEGG, kyoto encyclopedia of genes and genomes.

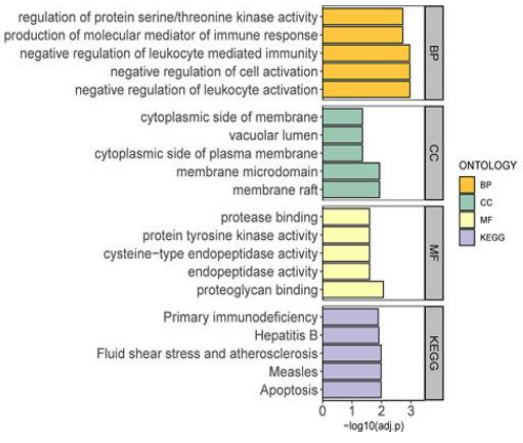

a)

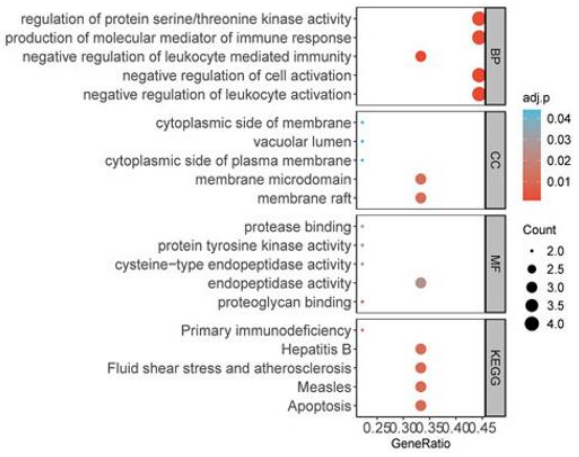

b)

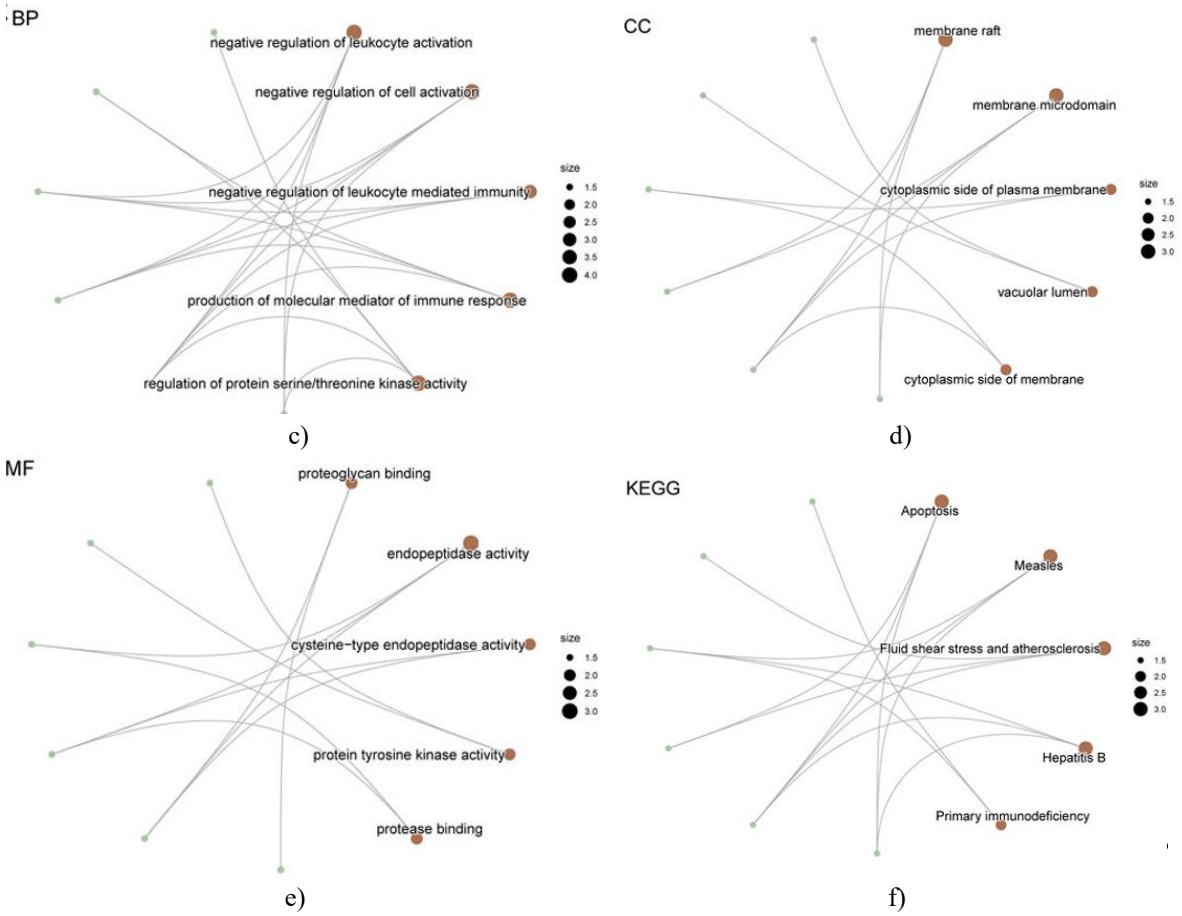

Figure 6. GO and KEGG Enrichment Analysis of Hub Genes. Bar charts (a) and bubble plots (b) display the GO and KEGG enrichment results for the hub genes, including biological processes (BP), cellular components (CC), molecular functions (MF), and KEGG pathways, with terms shown on the y-axis. Network diagrams (c–f) illustrate the relationships between hub genes and enriched terms: BP (c), CC (d), MF (e), and KEGG (f). In these diagrams, brown nodes indicate functional terms, green nodes represent genes, and connecting lines show associations between genes and terms. In the bubble plots, bubble size reflects the number of associated genes, while color intensity indicates adjusted p-value—red denotes smaller adj. p-values and blue denotes larger adj. p-values. GO and KEGG terms were considered significant if adj. p-value < 0.05 and FDR (q-value) < 0.25, with Benjamini–Hochberg correction applied.

Biological processes (BP)

GO enrichment revealed that hub genes play critical roles in AML-related biological processes, including negative regulation of leukocyte activation and immune-mediated pathways. These processes are central to understanding how APS may enhance immune surveillance within the AML microenvironment, supporting the elimination of leukemic cells. Modulation of immune activation is vital for strengthening the body's anti-leukemia response. Hub genes were also involved in regulating protein serine/threonine kinase activity, a key mechanism in signaling pathways that control cell proliferation and apoptosis in AML.

Molecular functions (MF)

Analysis of molecular functions indicated that hub genes are significantly associated with proteoglycan binding and endopeptidase activity. Proteoglycan interactions can influence cell adhesion and migration, processes important for leukemia progression and metastasis. Endopeptidase activity contributes to proteolytic regulation, impacting both tumor development and immune cell activation. By affecting these molecular activities, APS may improve immune responses and potentially limit leukemic cell invasiveness.

Cellular components (CC)

Hub genes were enriched in membrane rafts and vacuolar lumen, structures essential for immune cell function. Membrane rafts, as specialized microdomains, facilitate signal transduction and immune activation, whereas the vacuolar lumen participates in autophagy and cellular debris processing. These components are particularly relevant in AML, as they support the activation of T cells and NK cells, which target and eliminate leukemic cells.

KEGG pathways

KEGG enrichment highlighted pathways directly linked to AML pathogenesis, including apoptosis, primary immunodeficiency, and hepatitis B. Apoptosis is especially important in leukemia treatment, as regulating cell death pathways affects leukemic cell survival and therapy response. Primary immunodeficiency pathways are relevant because many childhood AML cases involve immune system dysfunction. By influencing these pathways, APS may help restore immune function, enhance leukemic cell clearance, and potentially reduce relapse risk.

Validation of differential expression and ROC analysis

Expression levels of the nine hub genes (CASP3, PTPRC, ELANE, HMOX1, CHUK, FLT1, JAK3, CTSL, AURKA) were significantly different between PAML and control groups ($p < 0.05$). ROC curve analysis using the pROC package demonstrated high classification performance (AUC > 0.9) for six genes—PTPRC, HMOX1, CHUK, FLT1, CTSL, AURKA—while CASP3, ELANE, and JAK3 showed moderate performance (0.7 < AUC < 0.9) **(Figures 7a–7j)**.

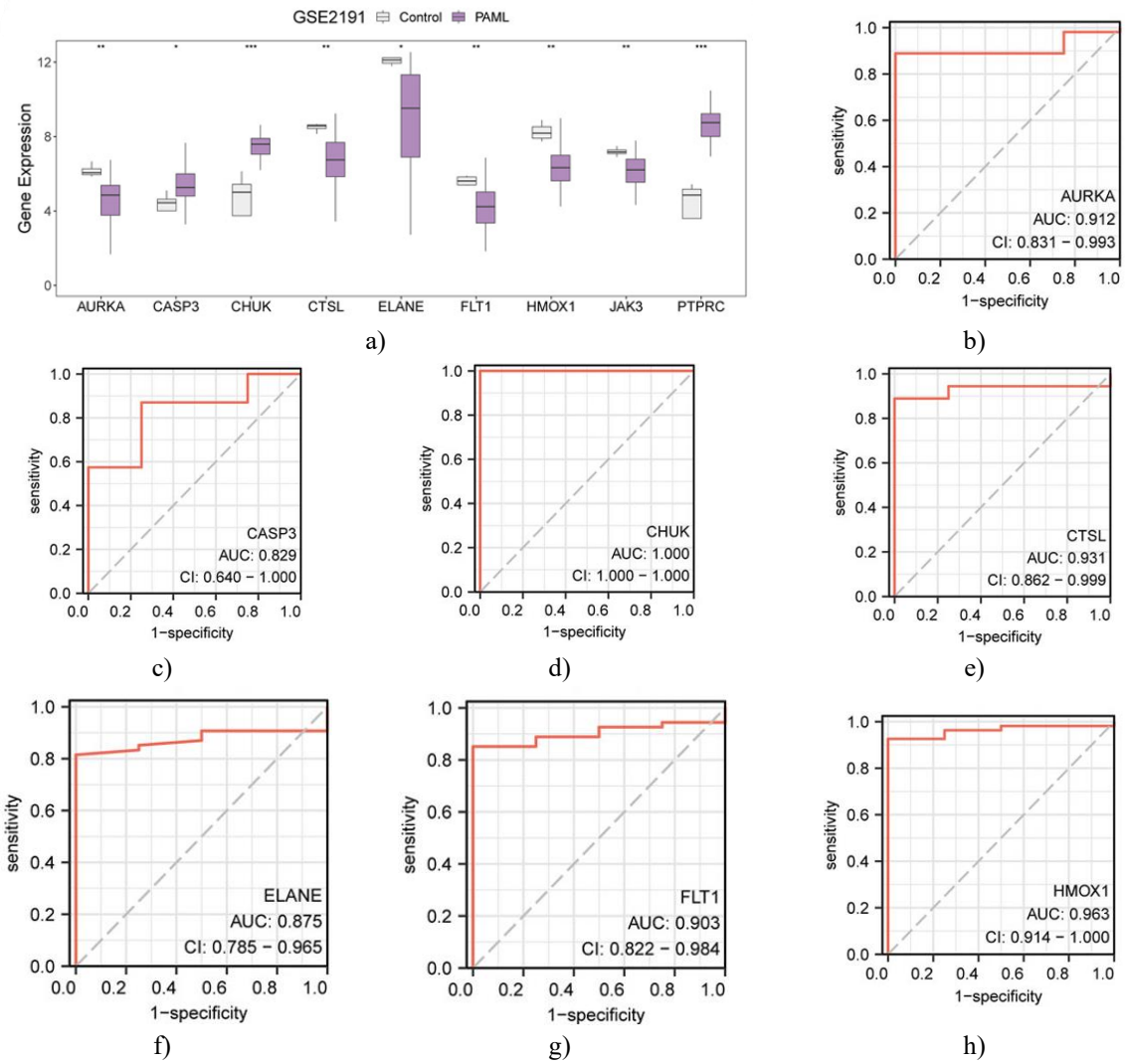

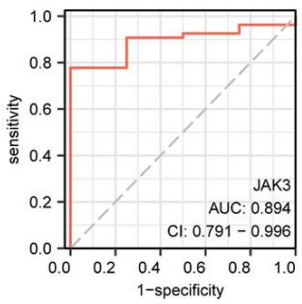

i)

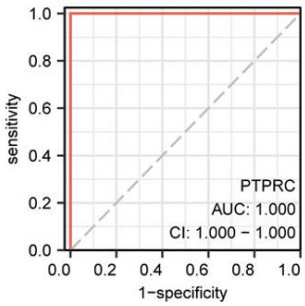

j)

Figure 7. Hub Gene Expression and ROC Analysis. Panel (a) displays a comparative analysis of hub gene expression levels between pediatric AML (PAML) samples and controls within the GSE2191 dataset. Panels (b–j) present ROC curves for individual hub genes: AURKA (b), CASP3 (c), CHUK (d), CTSL (e), ELANE (f), FLT1 (g), HMOX1 (h), JAK3 (Ii), and PTPRC (j). Significance levels are denoted as *p < 0.05, **p < 0.01, and ***p < 0.001. An AUC above 0.5 indicates that higher gene expression is associated with the event, with values approaching 1 representing stronger diagnostic reliability; AUCs from 0.7 to 0.9 indicate moderate predictive power, whereas AUCs exceeding 0.9 reflect high diagnostic accuracy. Gray indicates control samples, and purple represents PAML samples.

Hub gene Correlation and Functional Relationships

Correlation analysis among the nine hub genes revealed that HMOX1 and CTSL were most positively correlated (r = 0.584, p < 0.05), while JAK3 and CHUK exhibited the strongest negative correlation (r = −0.395, p < 0.05) **(Figure 8a)**. To further illustrate these associations, scatter plots were generated using ggplot2, highlighting the gene pairs with the highest positive and negative correlations **(Figures 8b and 8c).**

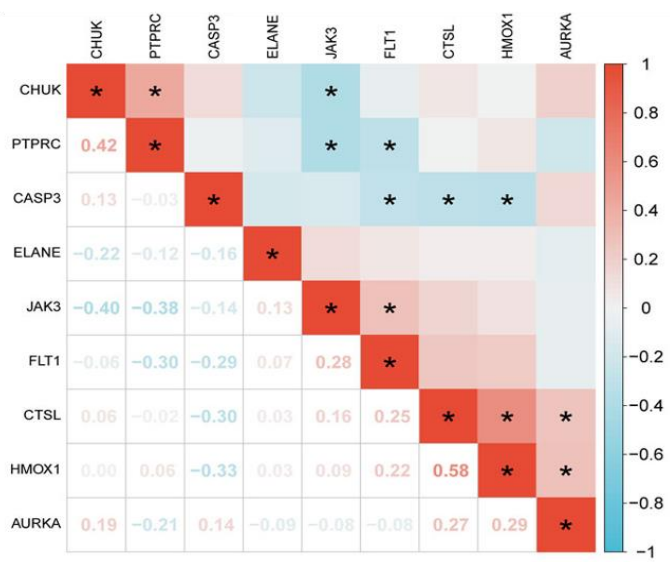

a)

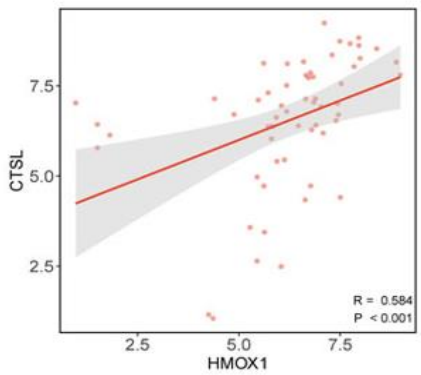

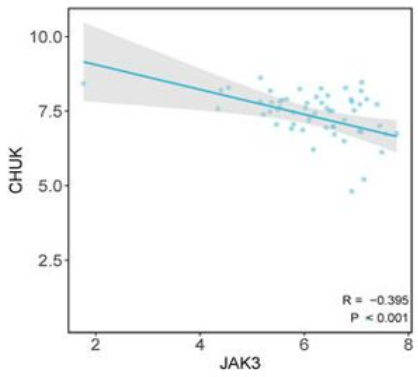

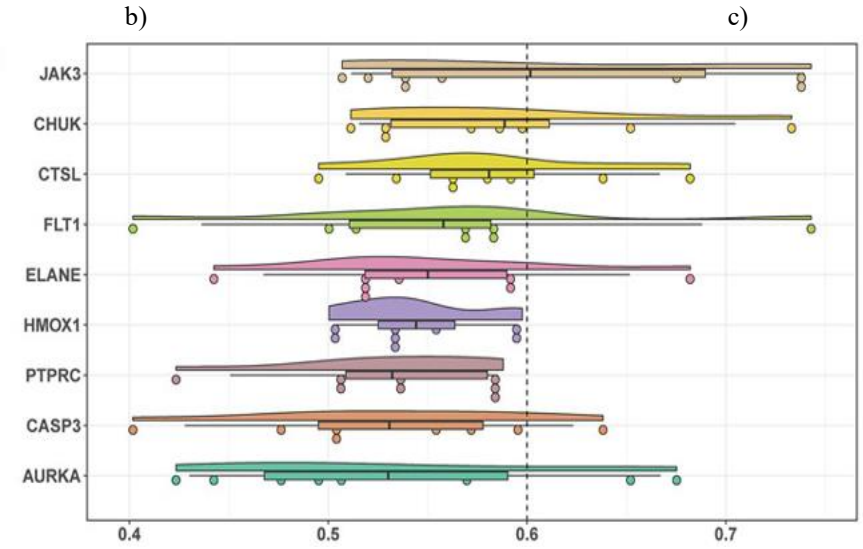

Figure 8. Correlation and Functional Similarity Analysis of Hub Genes. Panel (a) shows a heatmap of pairwise correlations among hub genes in the PAML and control groups from dataset GSE2191. Panels (b) and (c) illustrate scatter plots for the most strongly correlated gene pairs: HMOX1 versus CTSL (b) and JAK3 versus CHUK (Cc). Panel (d) presents a cloud rain plot depicting functional similarity ("Friends") among hub genes. Statistical significance is indicated by *$p < 0.05$. Correlation strength is categorized as follows: $|r| < 0.3$, weak or no correlation; $0.3 \leq |r| < 0.5$, weak correlation; $0.5 \leq |r| < 0.8$, moderate correlation.

In the group comparison plots, purple represents PAML samples and gray represents controls. In the correlation heatmap, red indicates positive correlation, blue indicates negative correlation, with color intensity reflecting correlation magnitude. Functional similarity analysis highlighted JAK3 as a key gene influencing critical biological processes in PAML **(Figure 8d)**.

Immune infiltration analysis in PAML

Immune cell infiltration was evaluated using the ssGSEA algorithm on GSE2191, revealing 15 immune cell types with significant abundance differences ($p < 0.05$), including activated B cells, activated $CD8^+$ T cells, activated dendritic cells, CD56^dim NK cells, effector memory $CD4^+$ T cells, eosinophils, mast cells, myeloid-derived suppressor cells (MDSCs), memory B cells, NK cells, NKT cells, neutrophils, and type 1, 2, and 17 T helper cells **(Figure 9a)**. A correlation heatmap of these 15 immune cell populations showed predominantly strong positive relationships, with MDSCs and neutrophils displaying the highest positive correlation ($r = 0.84$, $p < 0.05$) **(Figure 9b)**. Additionally, correlations between hub genes and immune cell abundance were visualized via a bubble plot **(Figure 9c)**, revealing numerous significant associations, with the strongest positive correlation observed between HMOX1 and neutrophils ($r = 0.592$, $p < 0.05$).

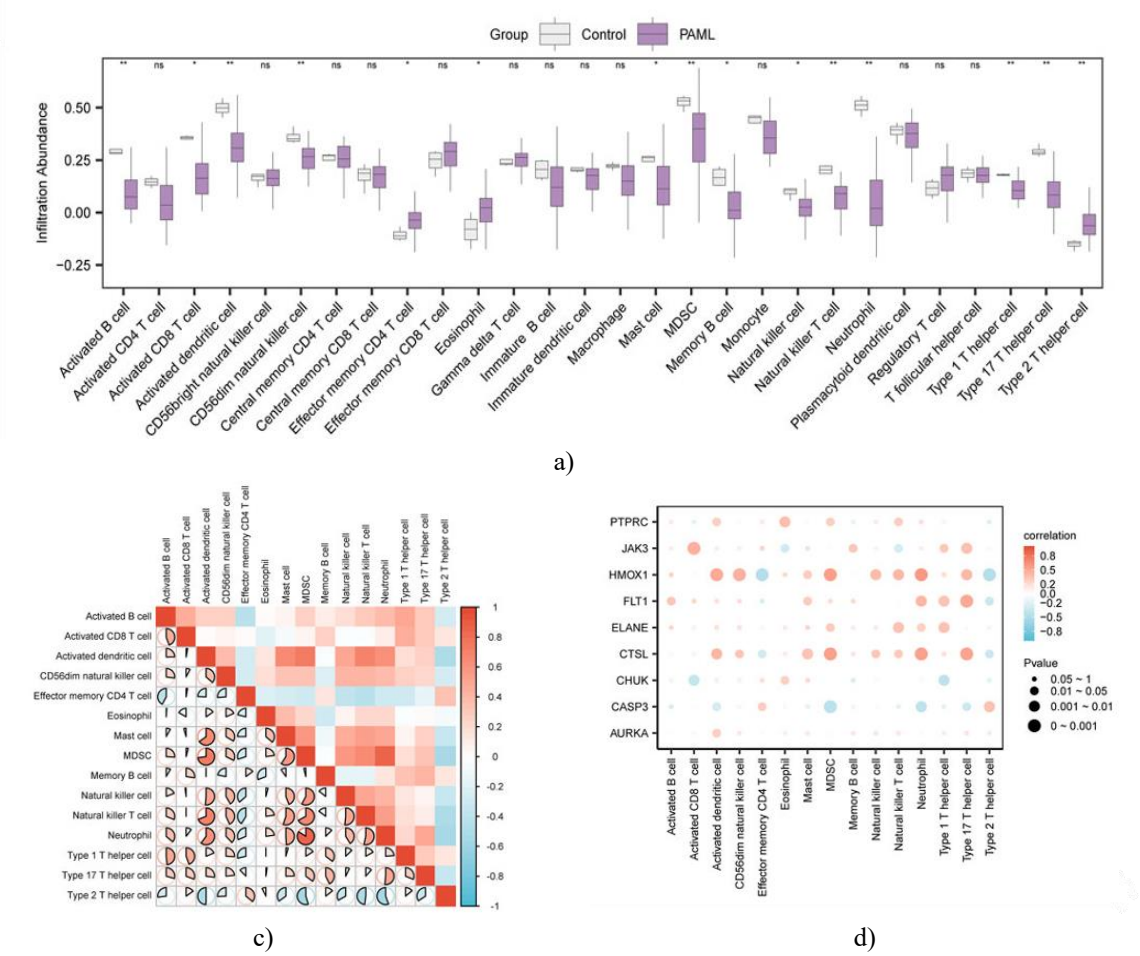

Figure 9. Immune Infiltration Assessment Using ssGSEA. Panel (a) compares immune cell abundances between control and PAML groups in dataset GSE2191. Panel (b) shows a heatmap of correlations among the infiltrating immune cells, while panel (c) illustrates the relationship between hub gene expression and immune cell infiltration through a bubble plot. Significance levels are indicated as ns ($p \geq 0.05$, not significant), *$p < 0.05$, and **$p < 0.01$. Correlation strengths were categorized as weak or none ($|r| < 0.3$), weak ($0.3 \leq |r| < 0.5$), moderate ($0.5 \leq |r| < 0.8$), and strong ($|r| \geq 0.8$). Gray represents control samples and purple indicates PAML samples. In correlation heatmaps, red signifies positive correlations and blue negative correlations, with color intensity reflecting correlation magnitude.

Acute myeloid leukemia (AML) is a malignant disorder arising from myeloid progenitor cells, primarily affecting leukocytes and distinct from erythrocytes, platelets, B cells, and T cells. Genetic mutations drive abnormal clonal expansion, leading to tumor formation and immune system dysregulation. AML represents roughly one-third of leukemia cases, yet treatment strategies have remained largely unchanged for decades, relying mainly on induction and remission chemotherapy. In this context, interventions that modulate immune function may offer novel therapeutic benefits.

This study explored the immunomodulatory potential of Astragalus polysaccharides (APS) in pediatric AML (PAML), emphasizing its ability to reshape the immune microenvironment and impact prognosis. PAML is often associated with high relapse rates and poor survival, underscoring the need for therapies beyond conventional chemotherapy [19, 20]. APS, with established immune-enhancing properties, emerges as a promising adjunct capable of strengthening anti-leukemic immune responses.

Treatment with APS was associated with significant alterations in the expression of key genes involved in apoptosis and immune regulation, including CASP3, PTPRC, and ELANE [21-24]. CASP3, a central mediator of programmed cell death, facilitates the elimination of malignant cells. Upregulation of PTPRC (CD45) indicates enhanced leukocyte function, critical for initiating robust anti-tumor immunity [25-28]. These gene expression changes suggest that APS may reprogram immune responses to more effectively target leukemic cells.

Protein-protein interaction (PPI) network analysis further highlighted the importance of immune-related hub genes, such as JAK3 and CHUK, both central to cytokine signaling and immune regulation. JAK3, in particular, is crucial for cytokine-mediated activation of immune cells, suggesting that APS may promote proliferation and activation of immune effector cells targeting AML [29, 30].

Immune infiltration analysis via ssGSEA revealed that APS treatment enhanced the presence of activated $CD8^+$ T cells, NK cells, and dendritic cells, all pivotal for anti-tumor responses [31]. These cells contribute both to direct cytotoxic effects and the orchestration of adaptive immunity through antigen presentation [32]. Correlation analyses identified significant associations between hub genes (JAK3, CTSL, HMOX1, FLT1) and various immune cell types, supporting GO and KEGG findings that APS influences pathways involved in leukocyte regulation, apoptosis, serine/threonine kinase signaling, and cytokine-mediated immune responses. These multi-target effects are consistent with the principles of traditional Chinese medicine, which emphasize broad, pathway-level modulation [33, 34]. Collectively, these results suggest that APS may enhance AML treatment efficacy and reduce relapse risk by modulating the tumor immune microenvironment.

While APS shows potential as an adjunct to conventional therapies, caution is warranted due to possible risks such as autoimmune reactions or cytokine release syndrome [35]. Further studies are necessary to optimize dosing, assess safety, and evaluate synergistic effects with other immunotherapies or targeted treatments, paving the way for personalized, immune-based strategies in pediatric AML.

Conclusion

This study highlights Astragalus polysaccharide (APS) as a promising adjunct therapy for pediatric acute myeloid leukemia (PAML). APS appears to enhance anti-tumor immunity by modulating immune cell infiltration and regulating key apoptotic and immune-related pathways, suggesting its potential to improve patient outcomes in this challenging disease. While these results are encouraging, further detailed mechanistic studies and well-designed clinical trials are essential to validate APS's therapeutic efficacy and ensure its safe integration into existing treatment regimens.

Study limitations

Several limitations of this study should be acknowledged. First, although we provided chemical formulas for APS, these represent simplified models of a highly complex polysaccharide. APS consists of multiple monosaccharide units, and the formulas presented do not fully capture its structural complexity, which may limit understanding of its biological activity. Future studies should focus on more detailed structural characterization to better define the molecular basis of APS's effects.

Second, the study relied on a publicly available dataset (GSE2191) that may not be fully representative of the global pediatric AML population. The dataset reflects a specific patient cohort, and its findings may not generalize to other populations. Expanding future analyses to include diverse patient cohorts and varying APS extraction methods would strengthen the applicability of these results.

Third, the precise molecular mechanisms through which APS exerts its biological effects remain incompletely understood. While bioinformatics analyses revealed APS-related gene expression changes, experimental validation is needed to elucidate the exact signaling pathways and interactions with immune cells and other molecular targets.

Additionally, the datasets used lacked detailed clinical information, such as treatment regimens, outcomes, and patient follow-up, which limits the immediate clinical translation of these findings. However, the primary aim of this study was to investigate APS's molecular effects rather than to establish clinical correlations.

Finally, future research should prioritize integrating datasets with comprehensive clinical information to validate these computational findings, better assess APS's therapeutic potential, and explore its practical applications in pediatric AML management.

Acknowledgments: The author was supported by the Fundamental Research Funds for China Medical University (2023JH2/10130004) and would like to thank all the colleagues and friends for their help.

Conflict of Interest: The authors declare that the research was conducted in the absence of any commercial or financial relationships that could be construed as a potential conflict of interest.

Financial Support: The author(s) declare that financial support was received for the research and/or publication of this article. The Fundamental Research Funds for China Medical University (2023JH2/10130004).

Ethics Statement: None

References

1. Hiroto I, Panetta JC, Pounds SB, Wang L, Li L, Navid F, et al. Sorafenib population pharmacokinetics and skin toxicities in children and adolescents with refractory/relapsed leukemia or solid tumor malignancies. Clin Cancer Res. 2019;25(24):7320-30.
2. Stevens AM, Miller JM, Munoz JO, Gaikwad AS, Redell MS. Interleukin-6 levels predict event-free survival in pediatric AML and suggest a mechanism of chemotherapy resistance. Blood Adv. 2017;1(19):1387-97.
3. Di Na, Liu FN, Miao ZF, Du ZM, Xu HM. Astragalus extract inhibits destruction of gastric cancer cells to mesothelial cells by anti-apoptosis. World J Gastroenterol. 2009;15(5):570-7.
4. Hopkins AL. Network pharmacology: the next paradigm in drug discovery. Nat Chem Biol. 2008;4(11):682-90.
5. Davis S, Meltzer PS. GEOquery: a bridge between the gene expression Omnibus (GEO) and BioConductor. Bioinformatics. 2007;23(14):1846-7.
6. Yagi T, Morimoto A, Eguchi M, Hibi S, Sako M, Ishii E, et al. Identification of a gene expression signature associated with pediatric AML prognosis. Blood. 2003;102(5):1849-56.
7. Ritchie ME, Phipson B, Wu D, Hu Y, Law CW, Shi W, et al. limma powers differential expression analyses for RNA-sequencing and microarray studies. Nucleic Acids Res. 2015;43(7):e47.
8. Kim S, Chen J, Cheng T, Gindulyte A, He J, He S, et al. PubChem in 2021: new data content and improved web interfaces. Nucleic Acids Res. 2021;49(D1):D1388-95.
9. Daina A, Michielin O, Zoete V. SwissTargetPrediction: updated data and new features for efficient prediction of protein targets of small molecules. Nucleic Acids Res. 2019;47(W1):W357-64.
10. Szklarczyk D, Gable AL, Lyon D, Junge A, Wyder S, Huerta-Cepas J, et al. STRING v11: protein-protein association networks with increased coverage, supporting functional discovery in genome-wide experimental datasets. Nucleic Acids Res. 2019;47(D1):D607-13.
11. Shannon P, Markiel A, Ozier O, Baliga NS, Wang JT, Ramage D, et al. Cytoscape: a software environment for integrated models of biomolecular interaction networks. Genome Res. 2003;13(11):2498-504.
12. Chin CH, Chen SH, Wu HH, Ho CW, Ko MT, Lin CY. cytoHubba: identifying hub objects and sub-networks from complex interactome. BMC Syst Biol. 2014;8 Suppl 4:S11.
13. Yang X, Li Y, Lv R, Qian H, Chen X, Yang CF. Study on the multitarget mechanism and key active ingredients of herba siegesbeckiae and volatile oil against rheumatoid arthritis based on network pharmacology. Evid Based Complement Alternat Med. 2019;2019:8957245.
14. Mi H, Muruganujan A, Ebert D, Huang X, Thomas PD. PANTHER version 14: more genomes, a new PANTHER GO-slim and improvements in enrichment analysis tools. Nucleic Acids Res. 2019;47(D1):D419-26.
15. Kanehisa M, Goto S. KEGG: kyoto encyclopedia of genes and genomes. Nucleic Acids Res. 2000;28(1):27-30.
16. Yu G, Wang LG, Han Y, He QY. clusterProfiler: an R package for comparing biological themes among gene clusters. OMICS. 2012;16(5):284-7.
17. Yu G, Li F, Qin Y, Bo X, Wu Y, Wang S. GOSemSim: an R package for measuring semantic similarity among GO terms and gene products. Bioinformatics. 2010;26(7):976-8.
18. Xiao B, Liu L, Xiang C, Wang P, Li H, Li A, et al. Identification and verification of immune-related gene prognostic signature based on ssGSEA for osteosarcoma. Front Oncol. 2020;10:607622.
19. Hu JX, Thomas CE, Brunak S. Network biology concepts in complex disease comorbidities. Nat Rev Genet. 2016;17(10):615-29.
20. Zhang C, Zhou W, Guan DG, Wang YH, Lu AP. Network intervention, a method to address complex therapeutic strategies. Front Pharmacol. 2018;9:754.
21. Porter AG, Jänicke RU. Emerging roles of caspase-3 in apoptosis. Cell Death Differ. 1999;6(2):99-104.
22. Hussar P. Apoptosis regulators Bcl-2 and caspase-3. Encyclopedia. 2022;2(4):1624-36.

23. Chua F, Laurent G. Neutrophil elastase: mediator of extracellular matrix destruction and accumulation. Proc Am Thorac Soc. 2006;3(5):424-7.
24. Cohen GM. Caspases: the executioners of apoptosis. Biochem J. 1997;326(Pt 1):1-16.
25. Li P, Wang W, Cao G, Pan T, Huang Y, Jin T, et al. PTPRC promoted CD8+ T cell mediated tumor immunity and drug sensitivity in breast cancer: based on pan-cancer analysis and artificial intelligence modeling of immunogenic cell death-based drug sensitivity stratification. Front Immunol. 2023;14:1145481.
26. Salmond R. Targeting protein tyrosine phosphatases to improve cancer immunotherapies. Cells. 2024;13(3):231.
27. Wong J, Berk E, Edwards R, Kalinski P. Receptor-type protein tyrosine phosphatases in cancer. Chin J Cancer. 2013;32(10):522-33.
28. Yang L, Klein S. Current trends and innovative approaches in cancer immunotherapy. AAPS PharmSciTech. 2022;23(4):102.
29. Yamaoka K, Kitamura T. Janus kinase 3 (JAK3): a critical conserved node in immunity disrupted in immune cell cancer and immunodeficiency. Int J Mol Sci. 2023;24(5):2977.
30. Li G, Brown J, Gao S, Liang S, Jotwani R, et al. The role of JAK-3 in regulating TLR-mediated inflammatory cytokine production in innate immune cells. J Immunol. 2023;211(4):587-98.
31. Li XF, Liu JQ, Zhang N, Zhou DX, Liu YK, et al. Decoding the immune microenvironment: unveiling CD8+ T cell-related biomarkers and developing a prognostic signature for personalized glioma treatment. Cancer Cell Int. 2024;24(1):331.
32. Smith AJ, et al. IL-18–Primed helper NK cells collaborate with dendritic cells to promote recruitment of effector CD8+ T cells to the tumor microenvironment. Cancer Res. 2021;81(12):3429-38.
33. Yang Q, Na J, Xue Z, Zhong L, Qin S, et al. Anticancer mechanism of Astragalus polysaccharide and its application in cancer immunotherapy. Pharmaceuticals (Basel). 2024;17(5):636.
34. Zhang L, Zhao X, Lu Z. Astragalus polysaccharides downregulate apoptosis in Hepg2 cells through the Wnt/β-catenin signaling pathway. Chin Tradit Herb Drugs. 2021;49(21):5155-60.
35. Cosenza M, Sacchi S, Pozzi S. Cytokine release syndrome associated with T-cell-based therapies for hematological malignancies: pathophysiology, clinical presentation, and treatment. Int J Mol Sci. 2021;22(14):7652.